Biochimica et Biophysica Acta, 944 (1988) 121–134
Elsevier

BBA 74146

Modelling the phase equilibria in two-component membranes of phospholipids with different acyl-chain lengths

John Hjort Ipsen and Ole G. Mouritsen

Department of Structural Properties of Materials, The Technical University of Denmark, Lyngby (Denmark)

(Received 2 May 1988)

Key words: Phospholipid bilayer; Binary mixture; Phase equilibrium; Hydrophobic thickness; Regular solution theory

A phenomenological model is proposed to describe the membrane phase equilibria in binary mixtures of saturated phospholipids with different acyl-chain lengths. The model is formulated in terms of thermodynamic and thermomechanic properties of the pure lipid bilayers, specifically the chain-melting transition temperature and enthalpy, the hydrophobic bilayer thickness, and the lateral area compressibility modulus. The model is studied using a regular solution theory made up of a set of interaction parameters which directly identify that part of the lipid–lipid interaction which is due to hydrophobic mismatch of saturated chains of different lengths. It is then found that there is effectively a single universal interaction parameter which, in the full composition range, describes the phase equilibria in mixtures of DMPC/DPPC, DPPC/DSPC, DMPC/DSPC, and DLPC/DSPC, in excellent agreement with experimental measurements. The model is used to predict the variation with temperature and composition of the specific heat, as well as of the average membrane thickness and area in each of the phases. Given the value of the universal interaction parameter, the model is then used to predict the phase diagrams of binary mixtures of phospholipids with different polar head groups, e.g., DPPC/DPPE, DMPC/DPPE and DMPE/DSPC. By comparison with experimental results for these mixtures, it is shown that difference in acyl-chain lengths gives the major contribution to deviation from ideal mixing. Application of the model to mixtures with non-saturated lipids is also discussed.

Introduction

A major effort in lipid research has been directed towards an understanding of the influence of lipid composition on global and local structural properties of membrane systems. The physical and thermodynamic states of lipid bilayers are of particular importance for the functioning of biological membranes [1,2], in which the lipid bilayer matrix serves as a solvent for various functional units of the cell, such as pumps, receptors, and enzymes. These units are usually functioning optimally, with respect to the living system, for a certain range of lipid composition of the membrane, by maintaining a certain molecular motional freedom ('fluidity') and lateral organization of the membrane components. The lipid diversity of biological membranes, however, makes it experimentally, as well as theoretically, very difficult to characterize the thermodynamic state of the lipid membrane and its associated phase equi-

Abbreviations: PC, phosphatidylcholine; PE, phosphatidylethanolamine; DLPC/PE, dilauroyl PC/PE; DMPC/PE, dimyristoyl PC/PE; DPPC/PE, dipalmitoyl PC/PE; DSPC/PE, distearoyl PC/PE; DEPC, dielaidoyl PC.

Correspondence: O.G. Mouritsen, Department of Structural Properties of Materials, The Technical University of Denmark, Building 307, DK-2800 Lyngby, Denmark.

libria. Within a reductionistic approach, the understanding of the phase equilibria in simple two-component lipid bilayers would constitute the first important step towards a description of complicated multi-component biological membranes. A rather complex phase behaviour can arise, however, even for binary lipid mixtures [3], of which the phosphatidylcholine/cholesterol system is a notoriously difficult example [4].

In this paper we shall be concerned primarily with mixtures where both components are saturated phospholipids. We shall focus on the effects of difference in acyl-chain length and type of polar head group on the phase behaviour. Our main conclusion is that it is possible, taking the elastic properties of the lipid bilayer sheet into account, to furnish a universal theoretical description of the full series of binary mixtures of diacylglycero-phosphatidylcholines such as DMPC/DPPC, DPPC/DSPC, DMPC/DSPC and DLPC/DSPC via a one-parameter thermodynamic minimal model. Furthermore, having the value of the 'single' model parameter available, we find that our modelling also has considerable quantitatively predictive power in relation to mixtures of lipids with different polar head groups, such as PC and PE.

A variety of experimental techniques have been used to elucidate the phase diagrams of phospholipid mixtures. The most commonly used techniques include calorimetry [5,6], magnetic resonance techniques [7–9], fluorescent-probe techniques [10,11], and X-ray and neutron-scattering methods [12,13], whereas for example freeze-fracture microscopy [14,15], dilatometry [16], and micromechanics [17] are less frequently used. Except for freeze-fracture methods, all of these experimental approaches to phase equilibria have the disadvantage of not being able to give direct information about the bulk equilibrium phase behaviour. Specifically, these techniques measure some local or global property (e.g., magnetic resonance line splitting or specific heat) and how this property varies in the temperature–composition plane. The phase lines are then subsequently inferred from the extent of broadening, or from possible anomalous features in the measured property. Obviously, any such relation between the profile of a globally measured quantity and the position of the phase lines, has to rely on a model whose validity has to be tested in each case. Similarly, local-probe techniques associating two-phase coexistence with superimposed spectral features have to come to grips with the relationship between the time-scales of the probe and the size of the domains on which it reports [18]. In the latter case, it becomes particularly troublesome when the lipid bilayers in question are subject to large thermal density fluctuations and cluster-formation phenomena [19], which on some time-scales for a local probe will look like phase coexistence, although it is not so in a strict thermodynamic sense. Turning then to the freeze-fracture techniques, these give, in principle, a direct 'picture' of the state of matter, and thus have the potential of revealing truly macroscopic phase separation. Such techniques are not without severe difficulties either. Firstly, they require rather harsh treatment of the sample and have poor temperature resolution. Secondly, they require that the coexisting domains are large enough to be visible. Considering all these fundamental difficulties with experimental approaches to phase equilibria in mixed-lipid systems, it should not be surprising to find that different experimental studies of the same mixture in some cases are interpreted in terms of rather different phase diagrams. Careful work along the lines of Davis and collaborators [18], combining several of the most powerful techniques, is currently the most promising way to make progress for mixed systems, although such work has not yet been reported for phospholipid mixtures.

On the theoretical side, the approach to phase equilibria in mixed phospholipid bilayers has been based on using two different classes of models: (i) phenomenological thermodynamic models, and (ii) microscopic interaction models. The study of the models in the first class (i) has progressed along two different routes. One, building on the Landau theory [20,21] which, in terms of a suitable chosen set of order parameters, describes the phase behaviour of the pure components as well as of the mixture; the other building on various classical solution theories [3,22], which take the known properties of the pure components as their input. The models of the second class (ii) have been investigated in great detail by means of various

approximation schemes [23–27], including the mean-field approximation, and, in somewhat lesser detail, by computer-simulation techniques [28]. Most of the more elaborate theoretical calculations for both classes of models have been successful, in the sense that the models contain enough unknown parameters to fit the experimental phase diagrams, with a new set of values of the parameters for each mixture in question. Our model study below belongs to the first class (i). It involves a phenomenological thermodynamic model which operates on the free-energy level and the model is dealt with within regular solution theory [3]. The advantage of our approach relative to previous theoretical work is that the model in a transparent and simple way incorporates the mechanical properties of the lipid bilayer membranes, and thus gains the virtue of being able to effectively describe a whole class of binary lipid mixtures by a single model parameter of specified value.

Model and regular solution theory

Our model of binary lipid mixtures is proposed within the framework of regular solution theory, in which the entropy of mixing is given by the entropy of an ideal mixture [3]. Regular solution theory can be considered an expansion of the free energy in terms of the thermodynamic densities in question. This expansion provides a simple and effective way of parametrizing experimental phase diagrams. Alternatively, regular solution theory can be constructed on the basis of assumptions about microscopic properties and thereby gives some insight into the molecular interactions in the lipid mixtures. Our regular solution theory includes both of these aspects.

As an input, the regular solution theory requires some basic properties of the two components and we shall first describe this input, which is of an experimental character. We shall assume that possible subtransitional and pretransitional effects can be ignored and shall only consider the pure phospholipid main first-order phase transition for each species. This transition takes the bilayer from a solid conformationally ordered state (g = gel) to a fluid conformationally disordered, liquid state (f = fluid) at some transition temperature, T_m. The molar free energy of the pure system can, for temperatures near T_m, be expressed as

$$\mu_o^\alpha(T) = \mu_o^\alpha(T_m) - S^\alpha(T - T_m) \tag{1}$$

where we have introduced the phase label $\alpha = f, g$. The reference chemical potential $\mu_o^\alpha(T_m)$ is unimportant for the phase behaviour, and the molar entropies S^α may be chosen such that

$$\Delta H(T_m) = T_m(S^f - S^g) \approx T_m \Delta S(T_m) \tag{2}$$

is fulfilled. $\Delta H(T_m)$ is the experimentally observed molar transition enthalpy. $\Delta H(T_m)$ and T_m constitute the thermodynamic input for the theory. We also introduce a thermomechanic input by considering the molar elastic energy μ_{el}^α due to a small uniform change, $\rho - \rho_o$, in the lateral density, ρ_o, of the bilayer

$$\mu_{el}^\alpha = \tfrac{1}{2} R^\alpha \left(\frac{\rho^\alpha - \rho_o^\alpha}{\rho_o^\alpha} \right)^2 = \frac{1}{2} \frac{R^\alpha}{(d_o^\alpha)^2} (d^\alpha - d_o^\alpha)^2 \tag{3}$$

In Eqn. 3, d^α is the hydrophobic thickness of the bilayer and R^α per unit area is the elastic area compressibility modulus [29]. The subscript 'o' refers to the non-perturbed equilibrium state of the pure lipid bilayer. Eqn. 3 holds because the bilayer volume can be considered as being approximately constant [30]. Hence we write

$$\mu_o^\alpha(T, d^\alpha) = \mu_o^\alpha(T, d_o^\alpha) + A^\alpha (d^\alpha - d_o^\alpha)^2 \tag{4}$$

where $A^\alpha = R^\alpha / 2(d_o^\alpha)^2$.

The entropy of mixing is assumed to be that of an ideal mixture

$$\Delta S_{mix}^\alpha = -RT \sum_i n_i^\alpha \ln n_i^\alpha + RT \left(\sum_i n_i^\alpha \right) \ln \left(\sum_i n_i^\alpha \right) \tag{5}$$

where n_i^α is the number of molecules of component i in phase α. In Eqn. 5, the summations are over the two components, and R is the gas constant. The assumption of ideal mixing is justified on grounds of extended similarity between the two components with respect to molecular size and packing capacity.

We then turn to the construction of the enthalpy of mixing which is the core of our modelling. We shall use a lattice-gas description by as-

suming that the two acyl chains of the lipids can be treated independently and associated with the sites of a triangular lattice. Within this framework, the nearest-neighbour interaction energy, e_{ij}, between components of type i and j ($i = 1, 2$; $j = 1, 2$) have contributions from hydrophobic as well as dispersive forces

$$e_{ij} = e_{ij}^{\text{hydro}} + e_{ij}^{\text{disp}} \tag{6}$$

In our choice of the form for the hydrophobic part, e_{ij}^{hydro}, we have been inspired by Mouritsen and Bloom's mattress model of lipid–protein interactions in membranes [31]. These authors consider mismatch between protein and lipid-bilayer hydrophobic thickness as important for the interaction between amphiphilic membrane components. Hence we write

$$e_{ij}^{\text{hydro}} = \gamma |d_i^\alpha - d_j^\alpha| \tag{7}$$

where γ is a positive energy constant representing the repulsion between components with a hydrophobic mismatch in lengths, $d_i^\alpha \neq d_j^\alpha$. The dispersive part, e_{ij}^{disp}, is of an attractive nature due to van der Waals forces. Since this contribution depends on the hydrophobic interface of contact between the components, it may be written in the simple form

$$e_{ij}^{\text{disp}} = -[\varepsilon - \varepsilon'(1-\delta_{ij})] \min(d_i^\alpha, d_j^\alpha) \tag{8}$$

where δ_{ij} is the Kronecker delta. The function $\min(d_i^\alpha, d_j^\alpha)$ measures the hydrophobic length of contact between components i and j and ε and ε' are positive energy constants. For a pure system, $e_{ii}^{\text{disp}} \propto -\varepsilon$ and it may be considered a system-independent property which measures the strength of the interchain van der Waals forces. For a mixed system, the nearest-neighbour interaction between different components is reduced to $\varepsilon - \varepsilon'$ which is a simple way of modelling the fact that defects and different packing properties affect the interaction between the hydrocarbon chains. ε', on the other hand, will depend on the head group and the degree of saturation. It should be emphasized that within the proposed model, the interaction energy, Eqn. 6, is phase dependent only through the length variables, d_i^α. The parameters γ, ε, and ε' are hence the only free parameters of the model.

The enthalpy of mixing can now be evaluated from the total interaction enthalpy

$$H^\alpha = z \sum_{i,j} \frac{n_i^\alpha n_j^\alpha}{n_1^\alpha + n_2^\alpha} e_{ij} \tag{9}$$

where z is the coordination number of the underlying lattice ($z = 6$ for the triangular lattice). The contribution from the pure components is

$$H_o^\alpha = z \sum_i n_i^\alpha e_{ii} \tag{10}$$

which is already included in $\mu_{o,i}^\alpha(T, d_{o,i}^\alpha)$. Hence the enthalpy of mixing takes the form

$$\Delta H_{\text{mix}}^\alpha = H^\alpha - H_o^\alpha$$

$$= z[(2\gamma + \varepsilon)|d_1^\alpha - d_2^\alpha| + 2\varepsilon' \min(d_1^\alpha, d_2^\alpha)] \frac{n_1^\alpha n_2^\alpha}{n_1^\alpha + n_2^\alpha} \tag{11}$$

Defining

$$B = z(2\gamma + \varepsilon), \quad C = 2z\varepsilon' \tag{12}$$

we observe that γ and ε cannot be separated in our theory. Consequently, we are left with only two free parameters, B and C.

The total free energy of our model can now be obtained by summation of the contributions Eqns. 4, 5, and 11

$$G = \sum_{\alpha = g,f} \sum_{i=1,2} [\mu_{o,i}^\alpha(T_{m,i}) + A_i^c(d_i^\alpha - d_{o,i}^\alpha)^2] x_i^\alpha$$

$$+ [B|d_1^\alpha - d_2^\alpha| + C \min(d_1^\alpha, d_2^\alpha)] \frac{x_1^\alpha x_2^\alpha}{x_1^\alpha + x_2^\alpha}$$

$$- RT \sum_{i=1,2} x_i^\alpha \ln x_i^\alpha + RT\left(\sum_{i=1,2} x_i^\alpha\right) \ln\left(\sum_{i=1,2} x_i^\alpha\right) \tag{13}$$

In Eqn. 13 we have introduced the usual molar fractions

$$x_i^\alpha = \frac{n_i^\alpha}{\sum_i n_i^\alpha}; \quad x_i = \sum_{\alpha = g,f} x_i^\alpha \tag{14}$$

Phase diagrams (T, x_i) can now be obtained from an analysis of the equilibrium conditions

$$\frac{\partial G}{\partial d_i^\alpha} = 0; \quad \mu_i^\alpha = \mu_i^{\alpha'}; \quad i = 1,2 \tag{15}$$

supplemented with the stability criterion in equilibrium

$$\frac{\partial^2 G}{\partial (d_i^\alpha)^2} > 0 \tag{16}$$

This analysis involves two steps. First, a minimization is performed of the free energy for fixed x_i leading to an expression for the equilibrium free energy. Second, this equilibrium free energy is decomposed according to the lever rule leading to the equilibrium values of the various concentration variables. From these values the phase boundaries are readily inferred.

Before closing the description of our model and regular solution theory it is instructive to compare the theory's part of the total non-ideal enthalpy, ΔH^α, cf. Eqn. 13,

$$\Delta H^\alpha = \sum_{i=1,2} A_i^\alpha (d_i^\alpha - d_{o,i}^\alpha)^2 x_i^\alpha + [B|d_1^\alpha - d_2^\alpha| + C \min(d_1^\alpha, d_2^\alpha)] \frac{x_1^\alpha x_2^\alpha}{x_1^\alpha + x_2^\alpha} \tag{17}$$

with that used in conventional versions of regular solution theory [3]

$$\Delta H^\alpha = -w^\alpha \frac{x_1^\alpha x_2^\alpha}{x_1^\alpha + x_2^\alpha} \tag{18}$$

where w^α is a phase-dependent effective interaction constant which is in fact a combination of pair interactions, $w^\alpha = [w_{11}^\alpha + w_{22}^\alpha - 2w_{12}^\alpha]/2$. Not only the second term of Eqn. 17 is of the form Eqn. 18, but also the first term in Eqn. 17, due to Eqns. 15 and 16, contains a contribution of this form. This contribution constitutes the dominant part of the A^α-term as far as the phase equilibria is concerned. Hence our regular solution theory may effectively be considered to be of the conventional form, Eqn. 18, but where the phase-dependent form of w^α has been identified in terms of basic system parameters.

Model parameters for pure lipid bilayers

The thermodynamic input to the model consists of the transition temperature T_m and the transition enthalpy $\Delta H(T_m)$ for each of the two components. The values of T_m and $\Delta H(T_m)$ are known quite accurately from experiments on a great variety of different lipid systems [32], and values pertinent for the present work are compiled in Table I. The value of $\Delta H(T_m)$ given in this table for DLPC is the one which Maybrey and Sturtevant [6] report as the total integrated heat obtained from $-4°C$ to $10°C$. This temperature interval contains the full thermal anomaly observed in the calorimetric scan which gives a trace which is distinctly different from that seen for the other lipids in Table I. We believe that this is the amount of heat relevant for the phase equilibria, rather than that obtained from a linear extrapolation of the $\Delta H(T_m)$-relationship obtained from the longer lipids [6].

The experimental information available on hydrophobic thicknesses of pure lipid bilayers and the corresponding average chain length is considerably more scarce and it often has to be inferred by combining measurements using a variety of techniques. This has been discussed thoroughly in a recent paper by Sperotto and Mouritsen [34] and it suffices here to make a few remarks. Firstly, the values of d^f and d^g in Table I refer to a hypothetical pure lipid bilayer state where a possible tilt angle of the $P_{\beta'}$ phase has been projected out. This hypothetical state is the relevant state to consider in a theory where it is the interface of hydrophobic lipid-lipid chain contact which enters the

TABLE I

THERMODYNAMIC AND THERMOMECHANIC PROPERTIES OF PURE LIPID BILAYERS

Lipid	T_m (°C)	$\Delta H(T_m)$ (kcal/mol)	d_o^g (Å)	d_o^f (Å)
DLPC	−1.8 [a]	4.77 [a]	33 [d]	20 [d]
DMPC	23.9 [a]	5.4 [a]	37 [d]	23 [d]
DPPC	41.4 [a]	8.7 [a]	41 [d]	26 [d]
DSPC	54.9 [a]	10.7 [a]	45 [d]	30 [d]
DMPE	49.5 [a]	5.8 [a]	37 [d]	23 [d]
DPPE	63 [b]	8.8 [c]	41 [d]	26 [d]

[a] Ref. 6. [b] Ref. 7. [c] Ref. 33. [d] Ref. 34.

energy expression. Only for bilayers with zero tilt angle is the length variable d_i^a identical to the hydrophobic bilayer thickness. Since in the other cases the average chain length and the bilayer thickness is trivially related via the tilt projection, we shall in the following, for the sake of simplicity, indiscriminately refer to d_i^a by using either term. Secondly, we have used the fact that the hydrophobic chain length does not depend on whether the head group is PC or PE.

The area compressibility modules have been measured accurately for only a very few different lipid membranes [35,36] and the values of A^f and A^g are not, within the experimental accuracy, significantly different for different saturated phospholipid bilayers. We shall therefore here, for all lipid bilayers considered, adopt the values $A^f = 4.8$ cal · mol^{-1} · Å^{-2} and $A^g = 8.6$ cal · mol^{-1} · Å^{-2} measured in micromechanical studies of large DMPC vesicles [35].

Determination of interaction parameters: Phase diagram of DMPC/DPPC mixtures

The model as presented in Eqn. 13 contains two at present unknown interaction parameters B and C. We shall in this section determine the values of these parameters by fitting the theoretically predicted phase diagram for DMPC/DPPC mixtures to that measured experimentally by calorimetry [6], cf. Fig. 1. It turns out that the value of B required to give a reasonable fit is much larger than the value of C. This implies that $d_1^a = d_2^a$ (lock-in) in the full composition range,

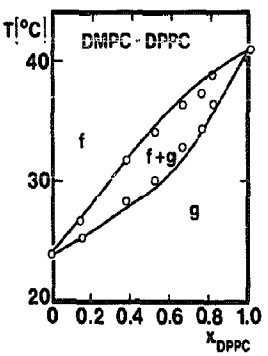

Fig. 1. Phase diagram of DMPC/DPPC mixtures. Theoretical prediction (——) and experimental data obtained by calorimetry (○) [6].

except for extreme mismatch. Consequently, the precise value of the parameter B is immaterial for the phase diagram calculation and it effectively drops out of the theory. We are therefore left with a single model parameter, C, to be determined. The physical reason for this is that lipids, in contrast to, e.g., integral membrane proteins [31], are soft and adapt easily to each other in order to avoid mismatch and high cost in hydrophobic energy.

In Fig. 1 is shown the best theoretical fit which is obtained for $C = 0.010$ kcal · mol^{-1} · Å^{-1} and $B \geq 0.15$ kcal · mol^{-1} · Å^{-1}. The fit is excellent and the theoretical phase lines are within the experimental confidence limits from calorimetry [6] in the full composition range. The experimental phase diagram for DMPC/DPPC mixtures has been studied by many other different experimental techniques and there is a general agreement about the position of the two-phase coexistence region. We therefore believe that the fit of our model to the DMPC/DPPC system is a very critical one with respect to the determination of the interaction parameter C. The fitting is sensitive to the value of C (but not to that of B for $B \gg C$), and C is accurate to within about 10%. The value of C is, in the limit of a pure lipid bilayer system, cf. Eqn. 8, similar to that used for modelling the phase transition properties via microscopic interaction models [24].

Phase diagrams of mixtures of DPPC/DSPC, DMPC/DSPC, and DLPC/DSPC

Having determined the value of the single parameter, C, of our theory we are now in a position to make theoretical predictions for other PC mixtures and study the influence of hydrophobic chain-length differences on the phase equilibria. In Figs. 2–4 our results are shown for mixtures of DPPC/DSPC, DMPC/DSPC, and DLPC/DSPC, together with the experimental data. It is immediately noted that the agreement in all three cases is very good and in fact astonishing in the light of the absence of free parameters!

We therefore conclude that our model has captured the essential physics in the interaction between acyl chains of different hydrophobic lengths and have shown how this interaction leads to

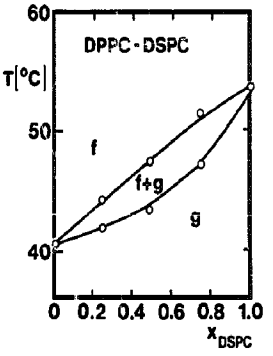

Fig. 2. Phase diagram of DPPC/DSPC mixtures. Theoretical prediction (———) and experimental data obtained by calorimetry (○) [6].

progressively less ideal behaviour as the chain-length difference is increased.

In the extreme case of the DLPC/DSPC system, the topology of the phase diagram has changed into that of peritectic behaviour. For this system, the available experimental data are not complete because of the proximity of the solidus line to the freezing point of water. Hence the

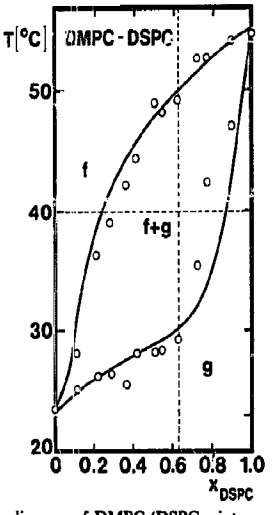

Fig. 3. Phase diagram of DMPC/DSPC mixtures. Theoretical prediction (———) and experimental data obtained by calorimetry (○) [6]. The vertical dashed line corresponds to a temperature scan at $x_{DSPC} = 0.63$ leading to results as shown in Figs. 5 and 7. The horizontal dashed line corresponds to a scan at constant composition at $T = 40\,°C$ leading to the results shown in Fig. 8.

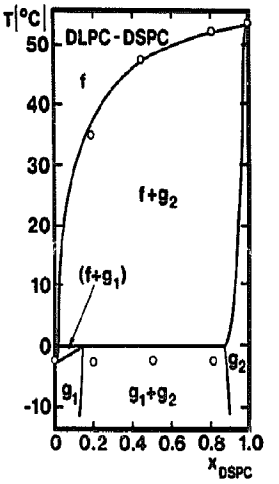

Fig. 4. Phase diagram for DLPC/DSPC mixtures. Theoretical prediction (———) and experimental data obtained by calorimetry (○) [6].

experiments can not discern whether there is peritectic behaviour or extreme coexistence asymmetry in the DLPC/DSPC mixture. The possibility of peritectic behaviour in this system has also previously been explored by other theoretical approaches [20,21]. It is noteworthy that the DLPC/DSPC mixture may constitute a system which permits an experimental determination of the value of the hydrophobic parameter, B, of our theory. For this mixture the three-phase line is sensitive to the value of B which could be determined indirectly by fitting to experimental data, if such data were more reliable than those reproduced in Fig. 4. As B is increased, the three-phase line moves down and the extent of the phases g_1 and g_2 diminishes. Our theory suggests that a somewhat more direct experimental assessment of B is made possible via the observation that for large mismatch the van der Waals chain-chain interaction is a strong competitor to the hydrophobic effect and lock-in of the acyl-chain lengths of the two species does not necessarily occur. In that case, Eqns. 13 and 15 imply the decoupled linear relations

$$d_1^\alpha = d_{0,1}^\alpha - \left(\frac{B}{2A_1^\alpha}\right)\frac{x_2^\alpha}{x_1^\alpha + x_2^\alpha}$$

$$d_2^\alpha = d_{0,2}^\alpha - \left(\frac{C-B}{2A_2^\alpha}\right)\frac{x_1^\alpha}{x_1^\alpha + x_2^\alpha} \qquad (19)$$

for $d_1^a > d_2^a$. A similar set of relations hold for $d_1^a < d_2^a$. Eqn. 19 turns out to hold in the one-phase regions g_1 and g_2 of the phase diagram in Fig. 4. Hence experimental measurement of the average acyl-chain length of the species separately gives access to B. Such a measurement should be possible by e.g. a ^{2}H-nuclear magnetic resonance experiment on a DLPC/DSPC mixture where the two lipid species are deuterated separately in turn.

Specific heat, membrane hydrophobic thickness, and membrane area

The excess specific heat is obtained from the free energy via the standard thermodynamic relation

$$C_P = \frac{\partial \Delta H}{\partial T} = \frac{\partial}{\partial T}\left[-T^2 \frac{\partial}{\partial T}\left(\frac{G(T)}{T}\right)\right] \tag{20}$$

To facilitate the numerical differentiation of the free energy and furthermore to provide a more direct way of comparing with experimental specific-heat data, we have convoluted the free energy curve with an 'instrumental window function', here taken to be a Gaussian of width σ. We then obtain a smoothened free energy $\tilde{G}$

$$\frac{\tilde{G}(T)}{T} = \int_0^\infty dT' \frac{G(T')}{T'} \exp[-(T-T')^2/2\sigma^2] \frac{1}{\sqrt{2\pi\sigma^2}} \tag{21}$$

From $\tilde{G}(T)$, the corresponding smoothened en-

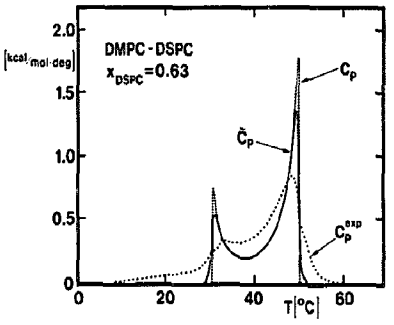

Fig. 5. Specific heat thermal profiles for DMPC/DSPC mixtures at composition $x_{DSPC} = 0.63$, cf. Fig. 3. Theoretical prediction $C_P(T)$ (- - - - -), theoretical prediction, $\tilde{C}_P(T)$, convoluted with a Gaussian of width 0.5 °C, Eqn. 21, (———), and experimental data, $C_P^{exp}(T)$, obtained by calorimetry (· · · · ·) [6].

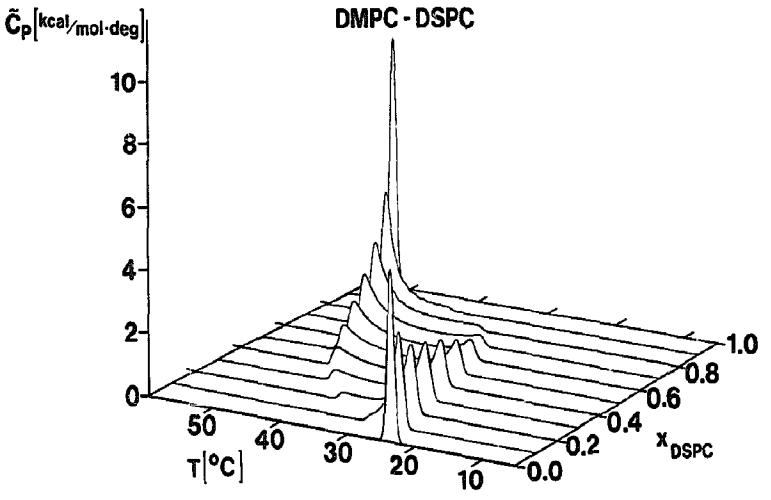

Fig. 6. Specific heat, $\tilde{C}_P$, vs. temperature and composition for DMPC/DSPC mixtures as predicted by the theory. The theoretical results are convoluted with a Gaussian of width 0.5 °C, Eqn. 21.

thalpy, $\Delta\tilde{H}$, can be obtained and finally, via Eqn. 20, the specific heat

$$\tilde{C}_P = \frac{2\Delta\tilde{H}}{T} + \frac{T}{\sigma^2}\tilde{G}(T) - \left(\frac{T}{\sigma^2}\right)^2 \int_0^\infty dT' \frac{G(T')}{T'}(T-T')^2$$

$$\times \exp[-(T-T')^2/2\sigma^2] \frac{1}{\sqrt{2\pi\sigma^2}} \qquad (22)$$

The thermal width of the window function is chosen to be $\sigma = 0.5\,^\circ$C.

In Fig. 5 is shown the specific-heat trace as obtained from the DMPC/DSPC mixture along a path of constant composition, $x_{DSPC} = 0.63$. Results are given for the directly calculated specific heat, $C_P(T)$, as well as for the convoluted one, $\tilde{C}_P(T)$. The theoretical results are compared with the experimental data, $C_P^{exp}(T)$, of Maybrey and Sturtevant [6]. The accordance between $\tilde{C}_P(T)$ and $C_P^{exp}(T)$ is satisfactory. Fig. 6 gives the full contour plot for $\tilde{C}_P(T)$ in the temperature-composition plane for the DMPC/DSPC mixture.

The theory of this paper gives access to a prediction of the variation of hydrophobic acyl-chain length (membrane hydrophobic thickness) with temperature and composition. In the case of lock-in, $d_1^\alpha = d_2^\alpha = d^\alpha$, and $A_1^\alpha = A_2^\alpha = A^\alpha$, Eqns. 13 and 15 imply in equilibrium a non-linear relation for d^α

$$d^\alpha = \frac{d_{0,1}^\alpha x_1^\alpha + d_{0,2}^\alpha x_2^\alpha}{x_1^\alpha + x_2^\alpha} - \frac{C}{A^\alpha} \frac{x_1^\alpha x_2^\alpha}{(x_1^\alpha + x_2^\alpha)^2} \qquad (23)$$

In Figs. 7 and 8 is shown the variation of d^α along the two paths of constant composition and temperature, respectively, as indicated on the DMPC/DSPC phase diagram in Fig. 3. For completeness, Fig. 8 also includes the specific-heat trace, $\tilde{C}_P(x_{DSPC})$. The constancy of d^α within each of the one-phase regions in Fig. 7 is a consequence of the assumption of temperature independence of the pure bilayer parameters, $d_{0,i}^\alpha$. In principle, the double-valued behaviour of d in the two-phase region could be measured in a scattering experiment or in a nuclear magnetic resonance experiment where the superimposed contributions to the first moment of the resonance lines [37] can be related to orientational order parameters and bilayer thicknesses [38].

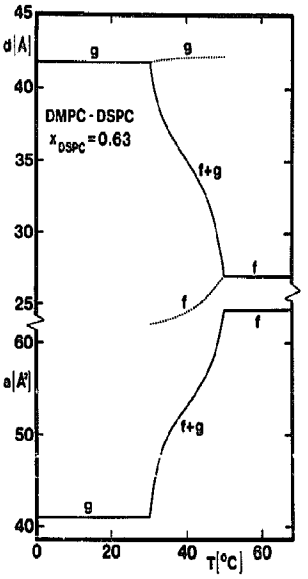

Fig. 7. Temperature variation of membrane hydrophobic thickness, d, and membrane area per molecule, a, for DMPC/DSPC mixtures at composition $x_{DSPC} = 0.63$, cf. Fig. 3, as predicted by the theory (———). The separate thicknesses of the f and g phases in the f+g coexistence region are denoted by (- - - - - -).

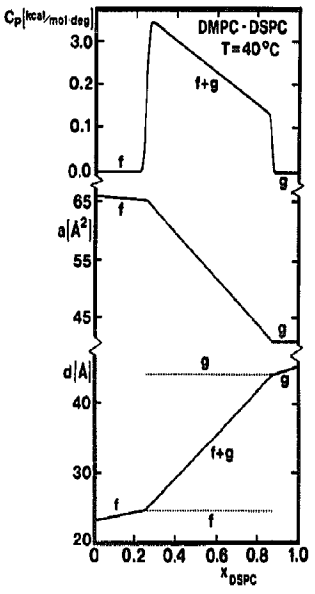

Fig. 8. Variation with composition, x_{DSPC}, of specific heat, $\tilde{C}_P$, membrane hydrophobic thickness, d, and membrane area per molecule, a, for DMPC/DSPC mixtures at temperature $T = 40\,^\circ$C, cf. Fig. 3, as predicted by the theory (———). The separate thicknesses of the f and g phases in the f+g coexistence region are denoted by (- - - - - -).

The approximation of constant volume gives rise to a simple temperature-independent reciprocal relationship between membrane hydrophobic thickness, d, and membrane area per molecule, a,

$$\tfrac{1}{2}da = v \qquad (24)$$

v is the specific hydrophobic volume of the lipids. By assigning a cross-sectional area of 40.8 Å^2 to the all-*trans* configuration of gel-state saturated PC bilayers [24], we have, via Table I, obtained the specific-volume data required to produce the membrane-area functions in Figs. 7 and 8. It should be noted that the membrane area in these figures refers to the cross sectional area per lipid molecule taken perpendicular to the long chain axis. In the case of a non-zero tilt angle, a in Figs. 7 and 8 should be appropriately projected to yield the true surface membrane area.

Phase diagrams of mixtures of lipids with different polar heads: DPPC/DPPE, DMPC/DPPE, and DMPE/DSPC

Most membranes consist of mixtures of lipids which have different kinds of polar heads. The class of binary mixtures PC/PE has been subject to particularly intensive experimental study [6–10,15,39–44]. The model and theory as presented in this paper has been devised to capture the non-ideality in the phase equilibria of lipid mixtures primarily due to differences in acyl-chain lengths. We shall now show that such a model built on the concept of hydrophobic mismatch has some predictive power even in the case of mixtures of saturated lipids which, in addition to chain-length differences, have different polar-head groups. It should be emphasized that the model parameters C and B are kept fixed for these calculations at their values used for PC/PC mixtures. Hence there are no new parameters to adjust.

We consider PC/PE mixtures and first make the observation that in the case of equal acyl-chain lengths, e.g., the DPPC/DPPE mixture, cf. Fig. 9, where our theory reduces to that of an ideal mixture, the theoretical prediction correlates rather well with the experimental data obtained from electron spin resonance [7]. The deviation for the solidus line at low DPPE concentrations may be due to a coupling between the planar $L_{\beta'}$ phase of DPPE and the rippled $P_{\beta'}$ of DPPC. Effects of this coupling are not accounted for in our theory.

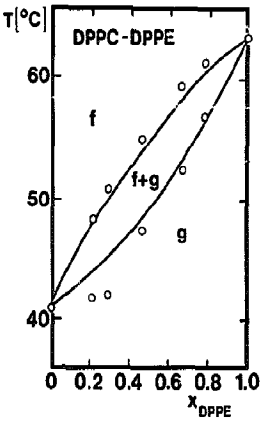

Fig. 9. Phase diagram of DPPC/DPPE mixtures. Theoretical prediction (———) which is that for an ideal mixture and experimental data obtained by electron spin resonance spectroscopy (○) [7].

Turning then to the DMPC/DPPE mixture in Fig. 10, a more pronounced non-ideal mixing behaviour is seen, and we note that our theory accounts for a major part of the asymmetric suppression of the solidus line. Again we attribute some of the deviation from the experimental data [7] as due to interference between planar and rippled gel phases.

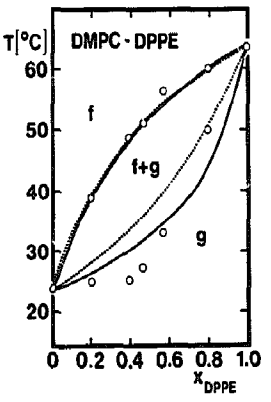

Fig. 10. Phase diagram of DMPC/DPPE mixtures. The theoretical prediction (———), ideal mixture curve (- - - - -), and experimental data obtained by electron spin resonance spectroscopy (○) [7].

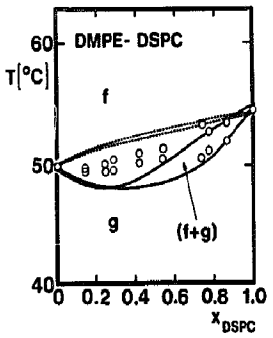

Fig. 11. Phase diagram of DMPE/DSPC mixtures. Theoretical prediction (———), ideal mixture curve (- - - - -), and experimental data obtained by calorimetry (○) [6].

Further remote from ideality is the phase equilibria of the DMPE/DSPC mixture in Fig. 11 where the non-ideal enthalpy of the theory even changes the topology of the phase diagram into that of azeotropic behaviour. The overall agreement with the calorimetric data is reasonable but we desist from making a closer quantitative comparison since the experimental phase diagram is still somewhat controversial and different experimental attempts [6,22,39] have led to phase diagrams which are mutually as different as the calorimetric and theoretical ones in Fig. 11.

Phase diagrams of mixtures with non-saturated lipids

We finally wish to point out that the model proposed in this paper may have an even more general sphere of application than outlined above. All of the mixtures with the phase diagrams in Figs. 1–4 and 9–11 were described by the same model parameters B and C. In particular, the fixed value of the parameter C reflected that the acyl chains of all these mixtures are fully saturated.

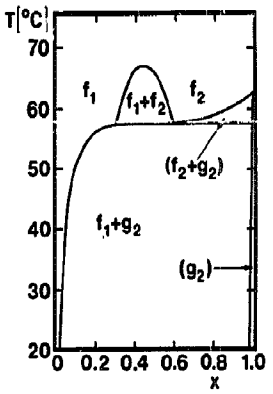

Fig. 12. Phase diagram for a hypothetical binary mixture of lipids with unsaturated acyl chains, e.g., DEPC/DPPE.

In order to account for non-saturation of the acyl chains, the value of C has to be modified. In Fig. 12 we show the theoretical prediction for a hypothetical binary lipid mixture which is characterized by $C = 0.047$ kcal $\cdot$ mol$^{-1} \cdot$ Å^{-1} and $B = 0.15$ kcal $\cdot$ mol$^{-1} \cdot$ Å^{-1}. The larger value of C in the non-saturated situation reflects a weaker van der Waals interaction between the two components, cf. Eqns. 8 and 12. The phase diagram in Fig. 12 displays monotectic behaviour and it is very similar, even quantitatively, to the experimental phase diagram for DEPC/DPPE mixtures [8].

Conclusions and Discussion

In this paper we have presented a general model and a regular solution theory for the phase equilibria in two-component bilayer membranes of phospholipids with different acyl chain lengths. The model identifies the difference in acyl chain lengths as a main determinant of the phase behaviour. Whereas the nature of the polar-head group is important for determining the phase transition temperature and the transition enthalpy of the pure system, the results presented here indicate that it is the chain-length difference which dictates the topology of the phase diagram of a mixed system. The model contains basically a single model parameter whose value is determined by fitting to experimental data for DMPC/DPPC mixtures, cf. Fig. 1. With this parameter values at hand and without further fitting, it is then shown that the model is capable of rather accurately reproducing the phase diagrams for other mixtures of saturated lipids, such as DPPC/DSPC, DMPC/DSPC, DLPC/DSPC, DPPC/DPPE, DMPC/DPPE, and DMPE/DSPC, cf. Figs. 2–4 and 9–11. Finally, by modifying the value of the model parameter to account for effects due to non-saturation, is found that the model can also describe the topology of phase diagrams of e.g., DEPC/DPPE mixtures, cf. Fig .12.

Hence we conclude that the proposed model and the regular solution theory is a very powerful and general approach to phase equilibria in binary lipid mixtures. It is likely that further investigation of the model may reveal an even larger sphere of applicability than discussed in the present work. The main virtue of the present approach, compared to conventional regular solution theories, is that it isolates a part of the non-ideal mixing enthalpy which can be parameterized in terms of mechanical properties of the pure lipid components, i.e. the hydrophobic acyl-chain lengths and the area compressibility modules. The part which is left after this parameterization, for mixtures of saturated lipids, turns out to be independent not only of the thermodynamic phase, but also of the lipid species in question. Another advantage of the present approach is that it leads to predictions not only about thermodynamic properties such as variations of specific heat across the phase diagram, cf. Figs. 5 and 6, but also about the thermal variation of membrane area and hydrophobic thickness, cf. Figs. 7 and 8. A disadvantage of the approach is that some of the pure lipid properties which the model requires as an input, such as hydrophobic average chain lengths and elastic modules, are at present not known with great accuracy.

A principal difficulty arises when the validity of a theoretical approach to phase equilibria in lipid membranes has to be tested against experimental data. Firstly, different experimental studies using different techniques on the same mixture do not always lead to the same phase diagram. In some cases, e.g. the DMPC/DSPC and DLPC/DSPC mixtures which we shall discuss below, even the topology of the phase diagram is controversial. Secondly, most experimental methods, e.g. calorimetry and magnetic resonance techniques, do not lead to a direct determination of the phase boundaries which have to be inferred from the characteristic variation of some, usually bulk, property of the mixture, e.g., the specific heat or moments of magnetic resonance lines. To relate the features in, e.g., a specific heat scan to the positions of the phase boundaries requires a model or a set of empirical rules. As shown in Fig. 5, peaks in the specific heat measured with a finite thermal resolution do not coincide with the phase boundary. The poorer the thermal resolution, the more the specific-heat peaks are displaced into the two-phase region. In the case of finite thermal resolution, the empirical rule of relating the phase boundaries to the inflection points of the specific heat scan [6] seems however rather reliable, cf. Fig. 5.

Another difficulty in comparing theoretical and experimental phase diagrams arises from the fact that our modelling does not account for the rippled $P_{\beta'}$ phase of the PC bilayers. This is particularly cumbersome for mixtures of PC and PE since the latter does not sustain a $P_{\beta'}$ phase. Rather, the $L_{\beta'}$ phase of the PE bilayers will promote the corresponding $L_{\beta'}$ phase of the PC bilayers and consequently push up in temperature the stability region of the $P_{\beta'}$ towards the fluid-solid coexistence region [19]. This is likely to affect the solidus line of this region and may explain the deviation between the theoretical and experimental phase diagrams in Figs. 9–11. Finally, it is possible that some of the experimental data is seriously affected by non-equilibrium properties [45,46].

The progressive deviation from ideal phase behaviour as is observed when the acyl-chain length difference in the mixture is increased, Figs. 1–4, eventually changes the topology of the phase diagram into one of peritectic behaviour, Fig. 4. The peritectic phase diagram can be considered as derived from a simple fluid-solid coexistence loop into which a solid-solid immicibility gap has intruded. As a result a three-phase line occurs. This is likely to be the case for the DLPC/DSPC mixture which is, however, difficult to analyze due to the controversial behaviour of the pure DLPC system [46]. In the case of the DMPC/DSPC mixture, the solid-solid (g_1-g_2) immicibility gap is strongly suppressed in the present model. The position of the critical point, however, depends very sensitively on the model parameter C. For $C = 0.015$ kcal · mol^{-1} Å^{-1}, the critical point has moved up into the fluid-solid coexistence region, i.e., it becomes an incipient critical point, and a peritectic phase diagram results. Using small-angle neutron scattering, Knoll et al. [47] recently found solid-solid immicibility in the DMPC(d_{54})/DSPC mixture around 5°C and surmised that the phase diagram is peritectic. The experimental data is too scarce however to permit a definite conclusion

about the low-temperature phase equilibria.

In conclusion, we wish to make some remarks regarding the concept of hydrophobic matching in lipid membranes. A number of experimental and theoretical studies of lipid-protein interactions in membranes (for a review, see Ref. 48) have suggested that matching between protein and lipid-bilayer hydrophobic thicknesses is an important regulator of membrane structure and dynamics as well as function. The present work on phase equilibria in lipid mixtures shows that the concept of hydrophobic matching maybe just as seminal for an understanding of the behaviour of the lipid matrix of biological membranes itself as it is for the interaction between lipid membranes and integral membrane proteins.

Acknowledgements

This work was supported by the Danish Natural Science Research Council under grant J. No. 5.21.99.52. An illuminating discussion with Jens Gert Rasmussen on the classification of phase diagrams is gratefully acknowledged.

References

1 Gordon, L.M. and Mobley, P.W. (1985) in Membrane Fluidity in Biology (Aloia, R.C. and Boggs, J.M., eds.), pp. 1–49, Academic Press, London.
2 Cullis, P.R., Hope, M.J., De Kruijff, B., Verkleij, A.J. and Tilcock, C.P.S. (1985) in Phospholipids and Cellular Regulation, Vol. I (Kuo, J.F., ed.), pp. 1–59, CRC Press, Boca Raton, FL.
3 Lee, A.G. (1977) Biochim. Biophys. Acta 472, 285–344.
4 Ipsen, J.H., Karlström, G., Mouritsen, O.G., Wennerström, H. and Zuckermann, M.J. (1987) Biochim. Biophys. Acta 905, 162–172.
5 Phillips, M.C., Ladbrooke, B.D. and Chapman, D. (1970) Biochim. Biophys. Acta 196, 35–44.
6 Mabrey, S. and Sturtevant, J.M. (1976) Proc. Natl. Acad. Sci. USA 73, 3862–3866.
7 Shimshick, E.J. and McConnell, H.M. (1973) Biochemistry 12, 2351–2360.
8 Wu, S.H. and McConnell, H.M. (1975) Biochemistry 14, 847–854.
9 Blume, A., Wittebort, R.J., Das Gupta, S.K. and Griffin, R.G. (1982) Biochemistry 24, 6243–6253.
10 Lee, A.G. (1975) Biochim. Biophys. Acta 413, 11–23.
11 Lenz, B.R., Barenholz, Y. and Thompson, T.E. (1976) Biochemistry 15, 4529–4537.
12 Ranck, J.L., Mateu, L., Sadler, d.M., Tardieu, A., Gulik-Krzywicki, T. and Luzatti, V. (1974) J. Mol. Biol. 85, 249–277.
13 Knoll, W., Ibel, K. and Sackmann, E. (1981) Biochemistry 20, 6379–6383.
14 Ververgaert, P.H.J.T., Verkleij, A.J., Elbers, P.F. and Van Deenen, L.L.M. (1973) Biochim. Biophys. Acta 311, 320–329.
15 Luna, E.J. and McConnell, H.M. (1978) Biochim. Biophys. Acta 509, 462–473.
16 Wilkinson, D.A. and Nagle, J.F. (1979) Biochemistry 18, 4244–4249.
17 Evans, E. and Needham, D. (1986) Faraday Discuss. Chem. Soc. 81, 267–280.
18 Morrow, M., Huschilt, J.C. and Davis, J.H. (1985) Biochemistry 24, 5396–5405.
19 Mouritsen, O.G. (1983) Biochim. Biophys. Acta 731, 217–221.
20 Priest, R.G. (1980) Mol. Cryst. Liq. Cryst. 60, 167–184.
21 Sugár, I.P. and Monticelli, G. (1985) Biophys. J. 48, 283–288.
22 Lee, A.G. (1978) Biochim. Biophys. Acta 507, 433–444.
23 Jacobs, R.E., Hudson, B.S. and Andersen, H.C. (1977) Biochemistry 16, 4349–4359.
24 Caillé, A., Pink, D.A., De Verteuil, F. and Zuckermann, M.J. (1980) Can. J. Phys. 58, 581–611.
25 Mondat. M., Georgallas, A., Pink, D.A. and Zuckermann, M.J. (1984) Can. J. Biochem. Cell Biol. 62, 795–802.
26 Scott, H.L. and Cheng, W.-H. (1979) Biophys. J. 28, 117–132.
27 Marčelja, S. and Wolfe, J. (1979) Biochim. Biophys. Acta 557, 24–31.
28 Pink, D.A. (1983) Can. J. Biochem. Cell Biol. 62, 760–777.
29 Sackmann, E. (1983) in Biophysics (Hoppe, W., Lohmann, W., Markl, H. and Ziegler, H., eds.), pp. 425–457, Springer-Verlag, Heidelberg.
30 Träuble, H. and Haynes, D.H. (1971) Chem. Phys. Lipids 7, 324–335.
31 Mouritsen, O.G. and Bloom, M. (1984) Biophys. J. 46, 141–153.
32 Silvius, J.R. (1982) in Lipid-Protein Interactions, Vol. II (Jost, P.C. and Griffith, O.H., eds.), pp. 239–281, Wiley, New York.
33 Waugham, D.J. and Keough, K.M. (1974) FEBS Lett. 47, 158–161.
34 Sperotto, M.M. and Mouritsen, O.G. (1988) Eur. Biophys. J. 16, 1–10.
35 Evans, E. and Kwok, R. (1982) Biochemistry 21, 4874–4879.
36 Evans, E. and Needham, D. (1987) J. Phys. Chem. 91, 4219–4228.
37 Huschilt, J.C., Hodges, R.S. and Davis, J.H. (1985) Biochemistry 24, 1377–1385.
38 Bloom, M. and Mouritsen, O.G. (1988) Can. J. Chem. 66, 706–712.
39 Blume, A. and Ackermann, T. (1974) FEBS Lett. 43, 71–74.
40 Mendelsohn, R. and Koch, C.C. (1980) Biochim. Biophys. Acta 598, 260–271.
41 Arnold, K., Lösche, A. and Gawrisch, K. (1981) Biochim. Biophys. Acta 645, 143–148.

42 Petrov, A.G., Gawrisch, K., Brzeziński, G., Klose, G. and Mögs, A. (1982) Biochim. Biophys. Acta 690, 1–7.

43 Silvius, J.R. (1986) Biochim. Biophys. Acta 857, 217–228.

44 Brauner, J.W. and Mendelsohn, R. (1986) Biochim. Biophys. Acta 861, 16–24.

45 Tsuchida, K., Ohki, K., Seki, T., Nozawa, Y. and Hara, I. (1987) Biochim. Biophys. Acta 898, 53–58.

46 Morrow, M.R. and Davis, J.H. (1987) Biochim. Biophys. Acta 904, 61–70.

47 Knoll, W., Schmidt, G. and Sackmann, E. (1983) J. Chem. Phys. 79, 3439–3442.

48 Mouritsen, O.G. (1987) in Physics in Living Matter (Benisvy, D., Diez, M., Malaprinas, A. and Marinoli, P., eds.), pp. 76–109, Springer-Verlag, Heidelberg.